Synthetic Metals 162 (2012) 1169–1176

Contents lists available at SciVerse ScienceDirect

Synthetic Metals

journal homepage: www.elsevier.com/locate/synmet

Multifunctional quinoxaline containing small molecules with multiple electron-donating moieties: Solvatochromic and optoelectronic properties

Dong Wook Chang[a], Seo-Jin Ko[b], Jin Young Kim[b,*], Liming Dai[c,*], Jong-Beom Baek[b,**]

[a] Department of Chemical Systematic Engineering, Catholic University of Daegu, 13-13, Hayang, Gyungbuk, 712-702, South Korea
[b] Interdisciplinary School of Green Energy/Low Dimensional Carbon Materials Center, Ulsan National Institute of Science and Technology, 100, Banyeon, Ulsan 689-798, South Korea
[c] Department of Macromolecular Science and Engineering, Case Western Reserve University, Cleveland, OH 44106, USA

ARTICLE INFO

Article history:
Received 26 February 2012
Received in revised form 3 April 2012
Accepted 13 April 2012

Keywords:
Quinoxaline
PVC
OLED
Optoelectronic properties
Solvatochromism

ABSTRACT

Two multifunctional quinoxaline containing small molecules (designated as: SD-1 and SD-2) composed of electron-donating (D) moieties both in vertical and horizontal directions to an electron-accepting (A) quinoxaline at the central position have been synthesized. In both SD-1 and SD-2, the dimethylaminobenzene (DMAB) and triphenylamine (TPA) groups were used as an electron-donor in the vertical direction, and dihexyloxy-functionalized TPA was adapted as an additional donor in the horizontal direction. The unique donor (D)–acceptor (A) structures around the central quinoxaline moiety impart special solvatochromic and optoelectronic features to the SD-1 and SD-2. Photovoltaic cells (PVCs) and organic light-emitting diodes (OLEDs) were fabricated from SD-1 and SD-2 by solution processing (*i.e.* spin-coating). While PVCs with a structure of ITO/PEDOT:PSS/SD-1 or SD-2:$PC_{71}BM$/Al show the power conversion efficiencies of 0.31% and 0.45%, respectively, OLEDs with a structure of ITO/PEDOT:PSS/SD-1 or SD-2/LiF/Al exhibit a maximum luminance (efficiency) of 7.42 cd/m^2 (0.034 cd/A) and 48.84 cd/m^2 (0.032 cd/A) with a turn-on voltage of 3.6 and 2.4 V, respectively. Furthermore, the Commission Internationale de L'Eclairage (CIE) chromacity coordinates of the OLED device with SD-2 were (0.67, 0.32), which are very close the CIE chromacity coordinates (0.67, 0.33) of National Television Society Committee (NTSC) for red color. Owing to their promising stimuli-responsive properties and device performances, these D–A molecules with unique structures can be considered as good candidates for multifunctional sensory and optoelectronic applications.

1. Introduction

Materials with combined electron-donor (D) and electron–acceptor (A) units connected *via* π-bridge(s) have been extensively studied for last two decades due to their potential applications in nonlinear optics (NLO) [1,2], organic thin film transistors (OTFTs) [3,4], organic light emitting diodes (OLEDs) [5–7], and photovoltaic cells (PVCs) [8–10]. One of the most significant features for the D-π–A molecules is their low band gaps induced by efficient electron delocalization *via* partial intramolecular charge transfer (ICT) between the donor and acceptor units along the conjugated molecular chain [10]. As a consequence, unique solvatochromic properties [11–13] have been observed for certain D–π–A molecules. Various electron donors, such as triphenylamine [14,15] carbazole [16,17] and fluorine [18,19], and acceptors, including benzothiadiazole [20,21] and quinoxaline [14,22,18] have been used for the design and synthesis of various functional D-π-A compounds. Meanwhile, thienyl, vinyl, and phenyl moieties have been utilized as the π-bridge between donor and acceptor units. Due to excellent electron-donating and nonaggregation properties associated with the non-planar molecular configuration [14,15], triphenylamine has been an important donor for many applications. Similarly, quinoxaline has been widely used in conjugated polymers as a strong electron–acceptor because of its high electron affinity originated from the two symmetric nitrogen atoms in the pyrazine ring [23–25].

Recently, solution-processable small molecular semiconductors have received great attention as active materials in optoelectronic devices, such as bulk heterojunction (BHJ) PVCs [26–29] and OLEDs [30–33]. Comparing with polymeric active materials, small molecules have several advantages, including their well-defined mono-dispersed chemical structures for reproducible materials synthesis and device performance as well as straightforward structure and property characterization. More specifically, great improvement in the PVCs power conversion efficiencies (up to 4.4% for diketopyrrollopyrrole (DPP) derivatives [34]) has been

* Corresponding authors.
** Corresponding author. Tel.: +82 52 217 2510; fax: +82 52 217 2509.
E-mail addresses: jykim@unist.ac.kr (J.Y. Kim), liming.dai@case.edu (L. Dai), jbbaek@unist.ac.kr (J.-B. Baek).

0379-6779/$ – see front matter © 2012 Elsevier B.V. All rights reserved.
http://dx.doi.org/10.1016/j.synthmet.2012.04.016

achieved with D–π–A small molecules since the important work reported by Roncali et al. in 2006 [35–37]. Along with the extensive studies on small molecules with D–π–A structures in PVCs [26–29,34–37], their applications in OLEDs have also been demonstrated to be promising with the recent availability of red emissive small molecules [30–33]. Although several multifunctional polymers, which can be used in PVCs and OLEDs as active materials simultaneously, have been investigated [38–41], there is no report on the multifunctional solution processable small molecules with the same purpose to our best knowledge. Therefore, it is interesting, though still quite challenging, to develop solution-processable small molecules with special D–π–A structures (*e.g.*, **SD-1**, **SD-2**) for optoelectronic device (*e.g.*, PVCs, OLEDs) and other applications.

Herein, we report the synthesis of two model compounds with electron-donating moieties in both vertical and horizontal directions to an electron-accepting quinoxaline core. It has been previously demonstrated that the synthesis of two-dimensional D-A structures around quinoxaline core in both *vertical* and *horizontal* directions and their applications for dye sensitized solar cells (DSSCs) [14] and OPVs [42]. The high population of active components in one molecule and the efficient formation of D-π-A structures through multi-directions are advantageous for optoelectronic applications. Our synthetic strategy involved that the dimethylaminobenzene (DMAB) and TPA connected with phenylene–vinylene linkage were used as donors in vertical direction for **SD-1** and **SD-2**, respectively. Consequently, dihexyloxy-functionalized TPA was adapted as an additional donor in the horizontal direction for both **SD-1** and **SD-2** (Fig. 1). A quinoxaline moiety has been selected as an acceptor due to the strong electron-withdrawing capability of its pyrazine ring and the ease with which structural modifications can be performed on 2 and 3-phenyl rings. In this study, we have investigated the interesting solvatochromic properties of **SD-1** and **SD-2** originated from their unique D-π-A conjugated structures around the quinoxaline central moiety, along with their potential applications in photovoltaic and electroluminescent devices. The observed interesting stimuli-responsive properties and device performance make these newly-synthesized small molecules with unique D–π–A structures attractive for multifunctional applications in various sensing and optoelectronic devices.

2. Experimental

2.1. Materials and measurements

1,2-Bis(4-dimethylaminophenyl)-1,2-ethandione was purchased from TCI. All other reagents and solvents were purchased from Aldrich. The compounds, **1** [43], **3** [14] and **5** [44] (Scheme 1) were synthesized according to literature procedures. Proton (^{1}H) and carbon (^{13}C) NMR spectra were recorded on a Varian VNMRS 600 spectrometer. UV–vis and photoluminescent spectra were measured using Perkin-Elmer Lambda 35 and LS 35, respectively. Cyclic voltammetry (CV) measurements were performed on a VersaSTAT3 potentiostat (Princeton Applied Research). For the CV measurements, a platinum electrode coated with a thin layer of small molecules and platinum wire were used as working and counter electrode, respectively. Ag wire was used as a pseudo-reference electrode with the ferrocene/ferrocenium redox pair as an external standard.

2.2. Syntheses and characterizations

4-(5,8-Dibromo-2-(4-(dimethylamino)phenyl)quinoxaline-3-yl)-*N*,*N*-dimethylbenzeneamine (**2**). **1** (0.50 g, 1.88 mmol) and 1,2-bis(4-dimethylaminophenyl)-1,2-ethandione (0.56 g, 1.88 mmol) were dissolved in 10 ml toluene and 10 ml acetic acid. The reaction mixture was heated under reflux overnight. After cooling to room temperature, the mixture was poured into distilled water and extracted with chloroform. The organic layer was separated and dried over $MgSO_4$ and filtered. The filtrate was dried on a rotary evaporator and the solid residue was recrystallized from chloroform/ethanol (1/4, v/v) mixture to give 0.71 g (72% yield) of **2** as a yellowish powder. MS (MALDI-TOF) *m*/*z* 524.88, calcd 524.02. ^{1}H NMR (600 MHz, $CDCl_3$): δ(ppm) = 7.75 (s, 2H), 7.71 (d, 4H), 7.67 (d, 4H), 3.01 (s, 6H). ^{13}C NMR (125 MHz, $CDCl_3$): δ(ppm) = 153.8, 151.2, 138.7, 131.7, 131.3, 126.1, 123.1, 111.6, 40.2.

***N*-(4-(4-(2-(4-(4-(Diphenylamino)styryl)phenyl)-5)-8-dibromoquinoxaline)-3-yl)-*N*-phenylamine** (**4**). **1** (0.15 g, 0.56 mmol) and **3** (0.42 g, 0.56 mmol) were dissolved in 10 ml toluene and 10 ml acetic acid. The reaction mixture was refluxed overnight. After cooling to room temperature, the mixture was poured into distilled water and extracted with chloroform. The organic layer was separated and dried over $MgSO_4$ and filtered. The filtrate was dried on a rotary evaporator and the solid residue was recrystallized from chloroform/ethanol (1/4, v/v) to give 0.35 g (65% yield) of **4** as an orange powder. MS (MALDI-TOF) *m*/*z* 977.97, calcd 978.81. ^{1}H NMR (600 MHz, $CDCl_3$): δ(ppm) = 7.90 (s, 2H), 7.71 (d, 4H), 7.50 (d, 4H), 7.39 (d, 4H), 7.25–7.28 (m, 8H), 7.11–7.14 (m, 8H), 7.02–7.06 (m, 8H). ^{13}C NMR (125 MHz, $CDCl_3$): δ(ppm) = 153.6, 147.7, 147.5, 139.2, 139.0, 136.6, 132.9, 131.0, 130.6, 129.6, 129.3, 127.6, 126.3, 126.1, 124.7, 123.6, 123.3, 123.2.

4-(Bis(4-hexyloxy)phenyl)aminobenzaldehyde 6). Phosphorous oxychloride (1.82 g, 11.72 mmol) was slowly added to dimethyl formamide (1.71 g, 23.40 mmol) at 0 °C. After stirring for 2 h, **5** (5.21 g, 11.70 mmol) in dichloroethane was added in one portion and the mixture was stirred at 90 °C for 2 h. The mixture was poured into ice water and neutralized with 2 M sodium hydroxide. The organic layer was separated and dried over $MgSO_4$ and filtered. The filtrate was dried on a rotary evaporator and the residue was purified by column chromatography (ethyl acetate/hexane, 1/10, v/v) to produce 3.60 g (65% yield) of **6** as a yellowish viscous liquid. MS (MALDI-TOF) *m*/*z* 473.09, calcd 473.29. ^{1}H NMR (600 MHz, $CDCl_3$): δ(ppm) = 9.75 (s, 1H), 7.62 (d, 2H), 7.11 (d, 4H), 6.88 (d, 4H), 6.84 (d, 2H), 3.95 (t, 4H), 1.78 (m, 4H), 1.47 (m, 4H), 1.35 (m, 8H), 0.92 (m, 6H). ^{13}C NMR (125 MHz, $CDCl_3$): δ(ppm) = 190.2, 156.9, 154.1, 138.6, 131.4, 128.0, 127.7, 116.7, 115.6, 68.3, 31.4, 29.3, 25.7, 22.6, 14.0.

4-(Hexyloxy)-(*N*-(4-hexyloxy)phenyl)-*N*-(4-vinylphenyl)benzenamine (7). Potassium *t*-butoxide (0.71 g, 6.33 mmol) was added to methyltriphenylphophonium iodide (2.86 g, 6.32 mmol) solution in 20 ml dry THF. After stirring for 15 min at room temperature, **6** (1.5 g, 3.17 mmol) in 10 ml dry THF was added dropwise. The solution was further stirred at room temperature for 6 h. Finally, the solid by-product was removed by filtration and the filtrate was concentrated and purified by column chromatography (ethyl acetate/hexane, 1/15, v/v) to produce 1.19 g (80% yield) of **7** as a yellow viscous liquid. MS (MALDI-TOF) *m*/*z* 471.13, calcd 471.31. ^{1}H NMR (600 MHz, $CDCl_3$): δ(ppm) = 7.21 (d, 2H), 7.03 (d, 4H), 6.87 (d, 2H), 6.81 (d, 4H), 6.62 (q, 1H), 5.57 (q, 1H), 5.08 (q, 1H). ^{13}C NMR (125 MHz, $CDCl_3$): δ(ppm) = 154.4, 147.5, 139.6, 135.3, 128.8, 125.8, 125.5, 119.3, 114.2, 109.9, 67.2, 30.5, 28.3, 24.7, 21.6, 13.0.

***N*-(4-((1E)-2-(5-(Bis(4-(hexyloxy)phenyl)amino)styryl)-2,3-bis(4-(dimethylamino)phenyl)quinoxaline-8-yl)vinyl)phenyl)-4-(hexyloxy)-*N*-(4-(hyxyloxy)phenyl)benzenamine (SD-1)**. **2** (0.10 g, 0.19 mmol), **7** (0.19 g, 0.40 mmol), palladium acetate (0.003 g, 0.01 mmol), potassium carbonate (0.067 g, 0.38 mmol), and tetra-*n*-butylammoniumbromide (0.062 g, 0.19 mmol) were mixed with 9 ml dry DMF. After degassing for 30 min with Ar, the mixture was heated under Ar at 90 °C for 2 days. The resultant black

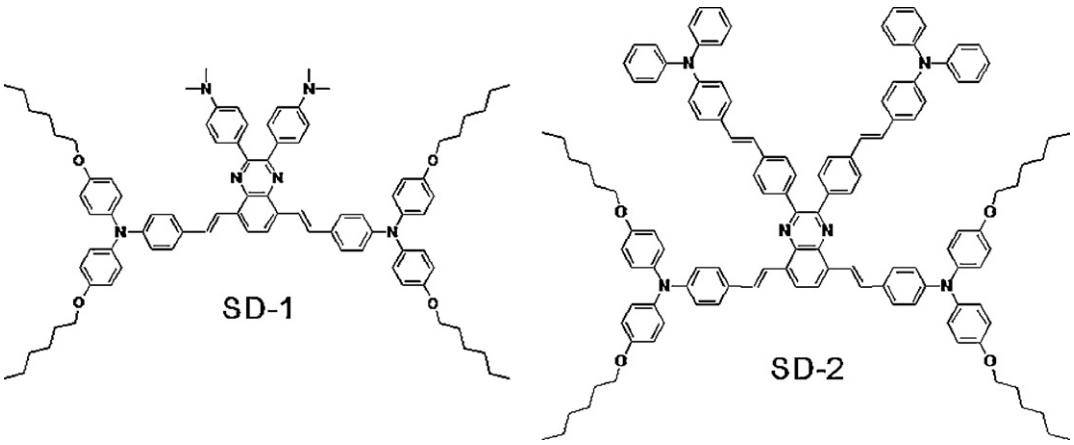

Fig. 1. Chemical structures of **SD-1** and **SD-2**.

mixture was diluted with chloroform and washed with 1 *N* HCl and brine. The organic layer was separated and dried over $MgSO_4$ and filtered. The filtrate was then concentrated and purified by column chromatography (chloroform/methanol, 10/1, v/v) to produce 0.11 g (70% yield) of SD-1 as a red powder. MS (MALDI-TOF) *m*/*z* 1307.59, calcd 1307.79. ^{1}H NMR (600 MHz, $CDCl_3$): δ(ppm) = 8.31 (d, 2H), 7.92 (s, 2H), 7.66 (d, 4H), 7.47 (d, 4H), 7.40 (d, 2H), 7.08 (d, 8H), 6.94 (d, 4H), 6.84 (d, 8H), 6.70 (d, 4H), 3.94 (t, 8H), 3.00 (s, 12H), 1.78 (m, 8H), 1.47 (m, 8H), 1.35 (m, 16H), 0.92 (m, 12H). ^{13}C NMR (125 MHz, $CDCl_3$): δ(ppm) = 154.5, 150.1, 149.7, 147.2, 139.6, 137.1, 133.0, 137.1, 132.0, 130.0, 129.4, 128.2, 126.7, 126.5, 125.6, 122.6, 120.5, 119.4, 114.2, 110.7, 67.2, 30.6, 28.3, 24.8, 21.6, 13.0. Anal. Calcd. For $C_{88}H_{102}N_6O_4$: C, 80.82%; H, 7.86%; N, 6.43%. Found: C, 80.98%; H, 7.77%; N, 6.31%.

***N*-(4-((1E)-2-(4-(5,8-Bis(4-(hexyloxy)phenyl)amino)styryl)-2-(4-(4-(diphenylamino)styryl)phenyl)quinoxaline-3-yl)phenyl)vinyl)phenyl)-*N*-phenylbenzenamine (SD-2)**. **4** (0.10 g, 0.10 mmol), **7** (0.10 g, 0.21 mmol), palladium acetate (0.002 g, 0.009 mmol), potassium carbonate (0.028 g, 0.20 mmol), and tetra-*n*-butylammoniumbromide (0.033 g, 0.10 mmol) were mixed with 6 ml dry DMF. After degassing for 30 min with Ar, the mixture was heated under Ar at 90 °C for 2 days. The resultant black mixture was diluted with chloroform and washed with 1 *N* HCl and brine. The organic layer was separated and dried over $MgSO_4$ and filtered. The filtrate was then concentrated and purified by column chromatography (chloroform/methanol, 10/1, v/v) to produce 0.11 g (70% yield) of SD-2 as a red powder. MS (MALDI-TOF) *m*/*z* 1759.61 (M^+), calcd 1759.96. ^{1}H NMR (600 MHz, $CDCl_3$): δ(ppm) = 8.30 (d, 2H), 8.02 (s, 2H), 7.69 (d, 4H), 7.38–7.50 (m, 18H), 7.26–7.28 (m, 4H), 7.00–7.13 (m, 28H), 6.95 (d, 4H), 6.84 (d, 8H). ^{13}C NMR (125 MHz, $CDCl_3$): δ(ppm) = 155.6, 150.8, 148.5, 147.5, 140.5, 138.5, 138.2, 138.1, 134.4, 131.3, 130.4, 130.0, 129.3, 129.0, 127.6, 127.5, 126.7, 126.4, 126.2, 124.6, 123.4, 123.1, 121.0, 120.2, 115.3, 68.3, 31.6, 29.7, 25.8, 22.6, 14.1. Anal. Calcd. For $C_{124}H_{122}N_6O_4$: C, 84.60%; H, 6.99%; N, 4.77%. Found: C, 84.42%; H, 6.82%; N, 4.61%.

Fabrication and characterization of photovoltaic cells (PVCs). The poly(3,4-ethylenedioxythiophene):poly(4-styrenesulfonate)

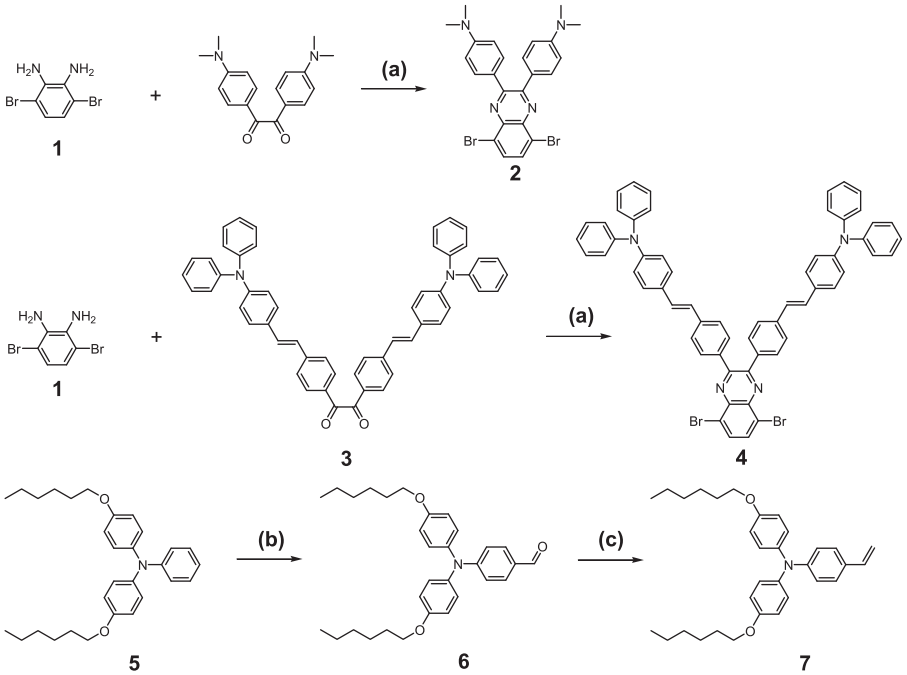

Scheme 1. Synthetic routes to quinoxaline-based core units, **2** and **4**, and dihexyloxy modified triphenylamine-based side units (**7**): (a) acetic acid/toluene, reflux, overnight; (b) $POCl_3$/DMF, dichloroethane, 90 °C, 2 h; (c) methyltriphenylphophine iodide, potassium *t*-butoxide, THF, 2 h.

(PEDOT:PSS) (Baytron PH) was purchased from H. C. Starck (Germany). [6,6]-phenyl-C71-butyric acid methyl ester ($PC_{71}BM$) was purchased from Electronic Materials (EM) Index Co., Ltd. PVCs with the structure of glass/indium-tin-oxide (ITO)/PEDOT:PSS/**SD-1** or **SD-2**:$PC_{71}BM$/Al were fabricated according to the following procedures. First, the glass substrates with ITO were cleaned with detergent, then ultra-sonicated in acetone and isopropyl alcohol in regular sequence, and subsequently dried in an oven overnight at 100 °C. PEDOT:PSS layer was spin-coated (after passing through a 0.45 μm filter) at 5000 rpm for 40 s on top of the ITO-coated glass followed by a bake at 140 °C for 10 min in air and then moved into a glove box. A mixed solution of [6,6]-Phenyl-C_{71}-butyric acid methyl ester ($PC_{71}BM$) with **SD-1** or **SD-2** in chlorobenzene was spin-coated at 2500 rpm for 60 s on top of the PEDOT:PSS layer. The device was then pumped down in vacuum (<10^{-6} T; 1 ~ 133 Pa), and a 100 nm thick Al electrode was deposited on top of the active layer. The deposited Al electrode defined the active area of the device as 13.5 mm^2. The whole device was then annealed at 120 °C for 10 min inside the glove box filled with nitrogen gas, in which the device performance was characterized by using a high quality optical fiber to guide the light from the solar simulator equipped with a Keithley 2635 A source measurement unit. The *J–V* curves were measured under air mass (AM) 1.5G illumination at 100 m Wcm^{-2} with mask. The measurements of incident photon to current efficiency (IPCE) were also conducted using an IPCE system (Model QEX7) from the PV Measurements Inc. (Boulder, CO). After collecting the IPCE data, the software also integrates the data with the AM 1.5G spectrum and reports the calculated J_{SC} value.

Fabrication and characterization of organic light emitting diodes (OLEDs). As is the case with the PVC fabrication, the glass substrates with ITO were first cleaned with detergent, then ultra-sonicated in acetone and isopropyl alcohol in regular sequence, and subsequently dried in an oven overnight at 100 °C. PEDOT:PSS layer was spin-coated (after passing through a 0.45 μm filter) at 5000 rpm for 40 s on top of the ITO-coated glass followed by a bake at 140 °C for 10 min in air. The **SD-1** or **SD-2** layer was then spin-cast from chlorobenzene solution (4 wt%) on top of the PEDOT:PSS layer at 1500 rpm and annealed at 120 °C for 10 min in nitrogen. Finally, the lithium fluoride (LiF) layer (1 nm) and Al layer (100 nm) were thermally evaporated onto the **SD-1** or **SD-2** surface at a deposition rate of 0.3 Å s^{-1}. The current density and luminance *versus* applied voltage characteristics were measured using a Keithley 2400 source measurement unit and a Konica Minolta spectro radiometer (CS-2000), respectively. All the device characteristics were measured under atmospheric conditions without additional device encapsulation/protection.

3. Results and discussion

3.1. Synthesis and characterization

The molecules, **SD-1** and **SD-2**, consisting of electron-accepting quinoxaline core and multiple electron-donating components, were synthesized in a moderate yield by the modified synthetic procedures illustrated in Schemes 1 and 2. For the preparation of **SD-1**, **1** and commecially available 1,2-bis(4-dimethylaminophenyl)-1,2-ethandione were reacted by the acid-catalyzed dehydration reaction to yield quinoxaline core **2**. For the synthesis of **SD-2**, **1** and **3**, prepared according to the previously reported procesure [14], were also reacted *via* the acid-catalyzed dehydration reaction to yield the modified quinoxaline core with vertically-orinted triphenylamine units, **4**. The electron-donating compound **7**, 4-(hexyloxy)-*N*-(4-hexyloxy)phenyl)-*N*-(4-vinylphenyl)benzenamine, was prepared

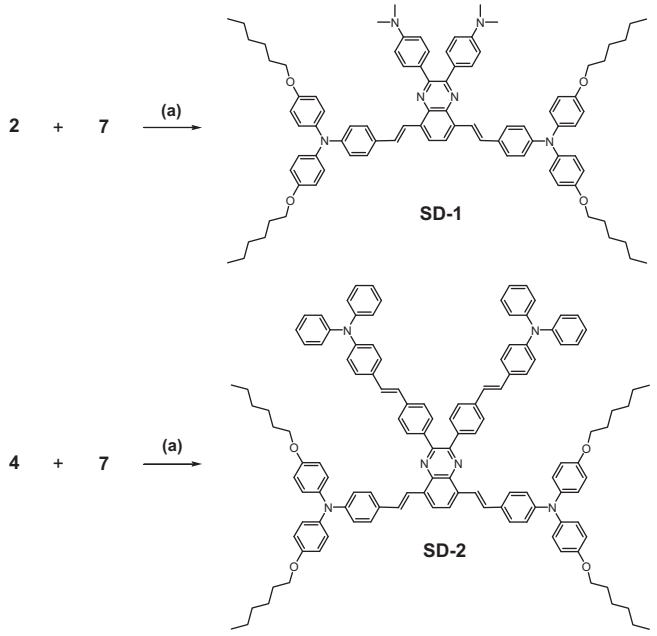

Scheme 2. Synthetic routs to **SD-1** and **SD-2**: (a) $Pd(OAc)_2$, Bu_4NBr, K_2CO_3, DMF, 90 °C, 48 h.

by three reactions from Ullman coupling reaction [45] for **5** through Vilsmeiyer formylation [46,47] for **6** to Wittig reaction [48] for the introduction of vinyl group (**7**). Then, **2** and **7** were coupled by Heck reaction to produce **SD-1** with multiple electron-donating components both in the vertical and horizontal directions. The Heck coupling reaction between **4** and **7** produced another target molecule **SD-2**, which also has multiple electron-donating components both in the vertical and horizontal directions. However, **SD-1** and **SD-2** contain different vertical electron-donors, *i.e.*, dimethylaminobenzene (DMAB) for **SD-1** and bulky triphenylamine derivatives for **SD-2**.

3.2. Optical and electrochemical properties

The optical properties of **SD-1** and **SD-2** were investigated by UV–vis absorption and photolumeniscent measurements. Dilute solutions of these molecules in chloroform were spin-cast on quartz plates. As shown in Fig. 2a, the **SD-1** solution and film exhibit two absorption peaks around 350 and 480 nm attributable to the π–π* transition and the intramolecular charge transfer (ICT), respectively. Similarly, **SD-2** also exhibits two peaks near 400 and 520 nm characteristic of the π–π* transition and ICT state, respectively. The PL spectra of **SD-1** and **SD-2** were also given in Fig. 2a, which showed the maximum PL intensities at 600 and 620 nm for **SD-1** and **SD-2**, respectively. No significant bathochromic shift in either UV–vis or PL spectra between the solution and film samples was observed from **SD-1** and **SD-2**. Therefore, the intramolecular interactions of **SD-1** and **SD-2** in solid state, which might cause the conformational changes of the molecules into more coplanar arrangements of conjugated structure, were almost negligible [49–51].

The electrochemical properties of **SD-1** and **SD-2** were investigated by cyclic voltammetry (CV). Fig. 2b shows the CV of **SD-1** and **SD-2** on a glassy carbon electrode with 0.1 M tetrabutylammonium hexafluorophosphate (Bu_4NPF_6) electrolyte in acetonitrile. The onset oxidation potentials E_{ox}^{on} of **SD-1** and **SD-2** were estimated to be 0.51 and 0.62 eV (*vs.* Ag/Ag^+), respectively. According to the empirical equation $E_{HOMO} = [-(E_{ox} - E_{FC}) - 4.8]$ eV[52], the highest occupied molecular orbital (HOMO) levels of **SD-1** and **SD-2** are estimated to be −4.94 eV and −5.03 eV, respectively. The calculated

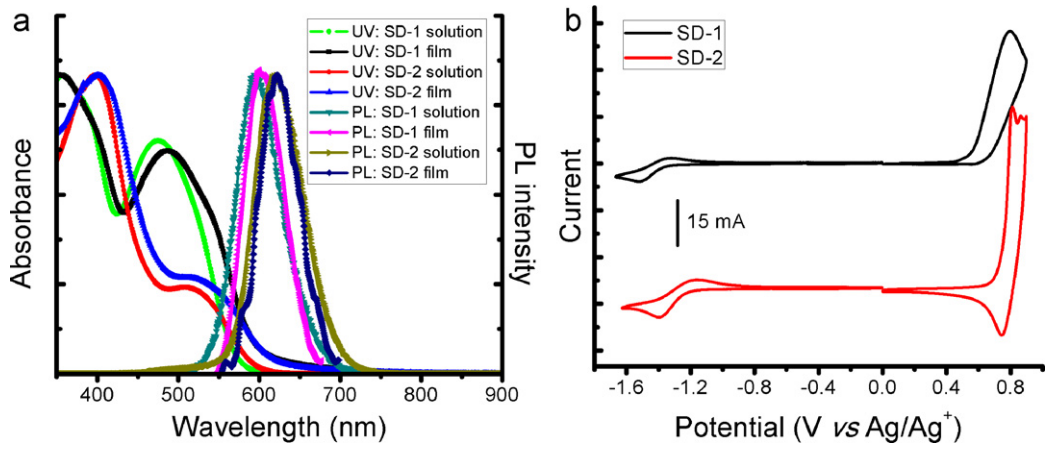

Fig. 2. (a) Normalized UV–vis and PL spectra of **SD-1** and **SD-2** in chloroform solutions at a concentration of 8.97 μM and films on quartz. The excitation wavelength for PL measurement is 300 nm; (b) cyclic voltammograms (CV) of **SD-1** and **SD-2** at a scan rate of 50 mV s^{-1}.

lowest unoccupied molecular orbital (LUMO) levels of **SD-1** and **SD-2** are −3.12 and −3.25 eV, respectively, using the onset reduction potentials. The calculated HOMO and LUMO levels of **SD-1** and **SD-2** matched well with those of $PC_{71}BM$ required for bulk heterojunction polymer solar cells (BHJ PSCs) (Table 1) [53].

3.3. Solvatochromic properties

When polarities of ground and excited states of a chromophore are different, a change in solvent polarities will change stabilization of the ground and excited states and the associated energy gap. As a result, variation in the peak position, intensity and shape of absorption spectra can be used to specify interactions between the solute and solvent molecules. The solvatochromic property is thus strongly dependent on the absorption and emission spectra with respect to solvent polarity. In general, molecules with a large change in their permanent dipole moment upon excitation exhibit a strong solvatochromism [54]. Therefore, a chromophore with D-π-A structures, in which the excited state is much stronger dipole than the ground state due to the intramolecular charge transfer on excitation, are more favorable to show solvatochromic properties [11–13,55].

To investigate solvatochromic properties, we first prepared the stock solutions of **SD-1** and **SD-2** in THF at a concentration of 0.73 mM. Then, 25 ml from each of the stock solutions was mixed with various solvents (2 ml) with different polarities for absorption and emission spectroscopic measurements. The final concentration of **SD-1** and **SD-2** during measurements was fixed at 8.97 μM. As shown in Fig. 3, the emission spectra of **SD-1** and **SD-2** show large solvatochromic effects whereas their absorption spectra are independent of solvent polarities (Fig. S1a and S1b). Both **SD-1** (Fig. 3a) and **SD-2** (Fig. 3b) show a relatively smaller Stokes shift in nonpolar solvents (*e.g.*, hexane) with respect to polar solvents (*e.g.*, methanol). They both show an increased bathochromic shift of emission band with increasing solvent polarity. Therefore, the solvatochromism of **SD-1** and **SD-2** indicates that the stabilization of the excited state is more efficient than that of ground state by the surrounding polar solvent molecules.

For the clear verification of solvent effects on the emissions of **SD-1** and **SD-2**, the plots of emission peak maxima *versus* Reichardt's solvent polarity parameters ($E_T(30)$) [54] are shown in Fig. S2. The maximum emission peak positions of **SD-1** and **SD-2** in various solvents with full width at half maximum (FWHM) were summarized in Table S1. Reichardt's polarity scale $E_T(30)$ OR E_T^N is widely acceptable for this purpose than the bulk solvent polarity parameters, such as the dielectric constant (ε) and refractive index (n), because it can take specific solvent–solute interactions into account. As shown in Fig. S2 and Table S2, the maximum emission peaks of **SD-1** and **SD-2** become more red-shifted in solvents with higher polarity values. These results suggest that general solvation effects are dominant in the solvents with lower polarity values while additional specific interactions, such as dipole–dipole relaxation, play important role in solvents with higher polarity values. Therefore, the unique solvatochromic properties of **SD-1** and **SD-2** could be attractive for sensing applications.

3.4. Photovoltaic properties

To investigate the photovoltaic properties of **SD-1** and **SD-2**, PVC devices with a structure of ITO/PEDOT:PSS/**SD-1** or **SD-2**:$PC_{71}BM$/Al were fabricated and their performance was tested under 100 mW/cm^2 AM 1.5 G illumination. The optimum ratios between small molecules and $PC_{71}BM$ in active layer of devices with the highest power conversion efficiency (PCE) are 1:2 and 1:4 for **SD-1** and **SD-2**, respectively. The resulting photovoltaic device performances were summarized in Table 2. The current–voltage curves (J–V) of the photovoltaic devices for **SD-1** and **SD-2** at the optimized condition are shown in Fig. 4a. The open-circuit voltage (V_{oc}), short-circuit current (J_{sc}), fill factor (FF) and PCE for the photovoltaic device of **SD-1** are 0.51 V, 2.05 mA/cm^2, 0.30 and 0.31%, respectively. Those of **SD-2** are 0.60 V, 2.48 mA/cm^2, 0.30 and 0.45%, respectively. The incident photon to current efficiency (IPCE)

Table 1
Optical and electrochemical properties of **SD-1** and **SD-2**.

Sample	$\lambda_{(nm)}^{abs}$ (nm)		$\lambda_{(max)}^{fluo}$ (nm)		E_{ox}^{on} (V)[a]	E_{on}^{red} (V)[a]	E_g^{cv} (eV)	E_g^{opt} (eV)
	Solution	Film	Solution	Film	HOMO (eV)[b]	LUMO (eV)[b]		
SD-1	350, 475	350, 487	600	605	0.51/−4.94	−1.31/−3.12	1.82	2.07
SD-2	398, 513	410, 520	621	623	0.60/−5.03	−1.15/−3.28	1.75	1.96

[a] Onset oxidation and reduction potentials were measure by cyclic voltametry.
[b] HOMO/LUMO = [−(E_{onset} − $E_{1/2(FC/FC+)}$)−4.8] eV, where $E_{1/2(FC/FC+)}$ = 0.37 V and 4.8 eV is the energy level of ferrocene below the vacuum.

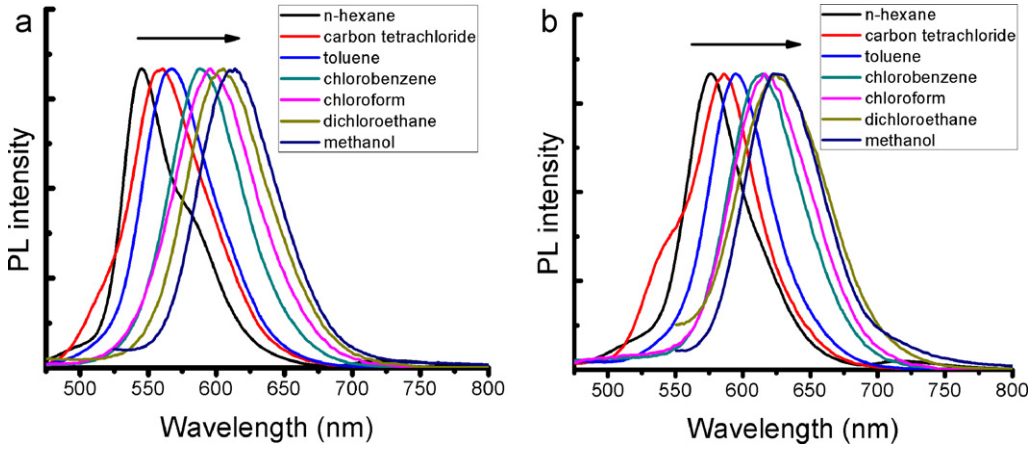

Fig. 3. Normalized photoluminescent spectra of (a) **SD-1** and (b) **SD-2** in various solvents. The concentration of **SD-1** and **SD-2** is 8.97 μM.

Table 2
Parameters for PVCs with optimized blend ratio of **SD-1** and **SD-2** with $PC_{71}BM$.

Materials	SD: $PC_{71}BM$	J_{sc} (mA/cm^2)	V_{oc} (V)	FF	PCE (%)
SD-1	1:2	2.05	0.51	0.30	0.31
SD-2	1:4	2.48	0.60	0.30	0.45

spectra of photovoltaic devices for both **SD-1** and **SD-2** were also shown in Fig. 4(b), which shows the similar IPCE curves from 350 to 700 nm and the higher maximum value of 25% was obtained for **SD-2**. On the other hands, the maximum IPCE value for photovoltaic devices based on **SD-1** was limited to 15%. The higher V_{oc} and short-circuit current J_{sc} of **SD-2** based photovoltaic device, which results in the high power efficiency, are likely to be related to deep-lying HOMO levels of **SD-2** (Table 1) and higher IPCE values of device **with SD-2** over 400–600 nm. These promising results from **SD-1** and **SD-2** based PVCs allow us to consider them as potential active materials for photovoltaic applications.

3.5. Electroluminescent properties

To investigate the electroluminescent (EL) properties, OLEDs with **SD-1** and **SD-2** as an emissive layer were fabricated by spin-coating. The device structure was glass/indium-tin-oxide (ITO)/PEDOT:PSS/**SD-1** or **SD-2**/LiF/Al, where PEDOT:PSS (poly(3,4-ethylenedioxythiopehe):poly(styrene sulfonate)) acts as the hole injecting and transporting layer, ITO and LiF/Al as anode and cathode, respectively. The EL spectra of devices were shown in Fig. 5a, which shows typical red emissive EL with peaks at 628 and 650 nm for **SD-1** and **SD-2**, respectively. Compared with their PL spectra in film, a large red shift of 23 and 28 nm was observed in EL spectra for **SD-1** and **SD-2**, respectively. The red-shift and broader peak in EL spectra compared with those in PL spectra are often observed [30,56]. They could be originated from the morphological changes of conjugated molecules during the annealing process for device fabrication [57–59]. The thermal annealing induces efficient molecular packing. The current–voltage (*I–V*), luminance–voltage (*L-V*) and current efficiency curves of devices with **SD-1** and **SD-2** are shown in Figs. 5b, 5c and 5d, respectively, and the detailed EL data are summarized in Table 3. As shown in Table 3, the nonoptimized OLED devices based on **SD-1** exhibit promising preliminary performances with a turn-on voltage of 3.6 V, a maximum luminance of 7.42 cd/m^2, and a maximum luminance efficiency of 0.034 cd/A with the Commission Internationale de L'Eclairage (CIE) (0.63, 0.36). For comparison, the OLED device fabricated from **SD-2** shows a turn-on voltage of 2.4 V, a maximum luminance of 48.84 cd/m^2, and a maximum luminance efficiency of 0.032 cd/A with CIE (0.67, 0.32), which is very close to the CIE chromaticity coordinates (0.67, 0.33) of National Television Society Committee (NTSC) for red color. Furthermore, OLED device performances are strongly influenced by the structural differences between **SD-1** and **SD-2**. The results

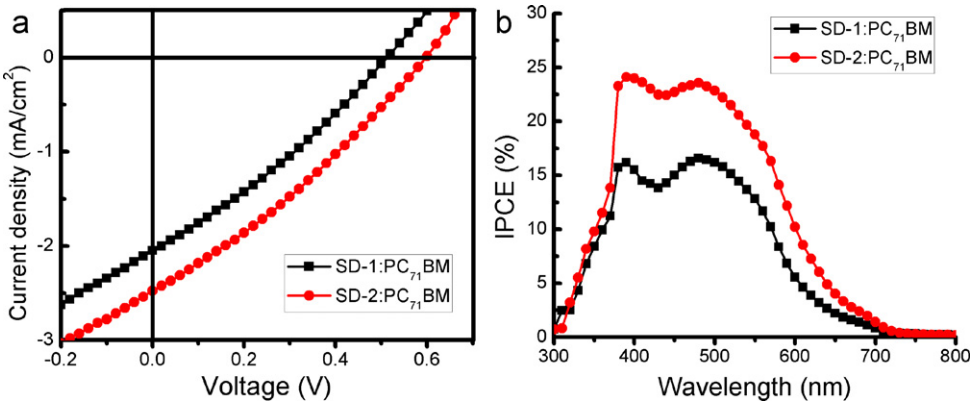

Fig. 4. (a) *J–V* characteristics and (b) IPCE spectra of photovoltaic devices with **SD-1** and **SD-2**.

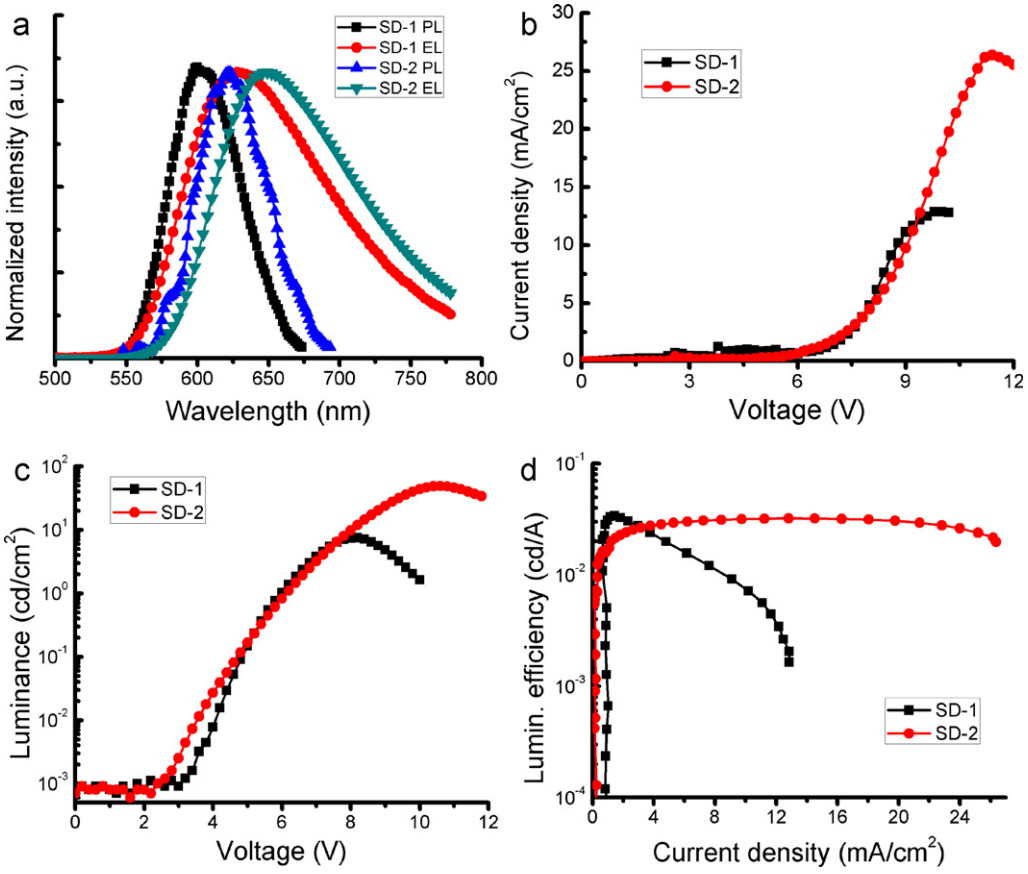

Fig. 5. (a) PL and EL spectra of **SD-1** and **SD-2**, (b) current–voltage (*I–V*), (c) luminance–voltage (*L–V*), and (d) luminance efficiency–current curves of electroluminescent device with **SD-1** and **SD-2**.

Table 3
OLED device performances of **SD-1** and **SD-2**.

Active material	Turn on voltage (V)	Maximum luminance (cd/m^2) [at Voltage]	Luminance efficiency (cd/A) [at Voltage]	PL peak wavelength (nm)	EL peak wavelength (nm)	CIE (x, y)
SD-1	3.6	7.42 [8.2 V]	0.034 [7.0 V]	605	628	0.63, 0.36
SD-2	2.4	48.86 [10.6 V]	0.032 [9.4 V]	622	650	0.67, 0.32

suggested that **SD-1** and **SD-2** could be used as an active material for red emissive OLEDs *via* simple solution processing.

4. Conclusions

We have synthesized two multifunctional quinoxaline-based molecules with D–π–A structures, *i.e.* **SD-1** and **SD-2**. Multiple electron-donating components, such as dimethylaminobenzene (DMBA) and bulky triphenylamine derivatives, were introduced both in the vertical and horizontal directions of an electron-accepting quinoxaline core. Due to the push-pull effect originated from the D–π–A structure and unique chemical structures, the **SD-1** and **SD-2** exhibit stimuli-responsive behaviors, such as solvatochromic properties. Furthermore, various devices such as photovoltaic cells (PVCs) and organic light-emitting diodes (OLEDs) have been fabricated *via* simple solution processing (*i.e.* spin-coating). Our preliminary results showed promising for these devices. Owing to their unique stimuli-responsive properties and device performances, **SD-1** and **SD-2** with D-π-A structures are potentially useful materials for sensory and optoelectronic applications.

Acknowledgments

We acknowledge financial support from the World Class University (WCU) program supported by National Research Foundation and Ministry of Education, Science and Technology of Korea.

Appendix A. Supplementary data

Supplementary data associated with this article can be found, in the online version, at http://dx.doi.org/10.1016/j.synthmet.2012.04.016.

References

[1] O. Ostroverkhova, W. Moerner, Chemical Reviews 104 (2004) 3267–3314.
[2] J.A. Delaire, K. Nakatani, Chemical Reviews 100 (2000) 1817–1846.
[3] T.T. Steckler, X. Zhang, J. Hwang, R. Honeyager, S. Ohira, X.H. Zhang, A. Grant, S. Ellinger, S.A. Odom, D. Sweat, Journal of the American Chemical Society 131 (2009) 2824–2826.
[4] R.D. Champion, K.F. Cheng, C.L. Pai, W.C. Chen, S.A. Jenekhe, Macromolecular Rapid Communications 26 (2005) 1835–1840.
[5] G. Hughes, M.R. Bryce, Journal of Materials Chemistry 15 (2004) 94–107.
[6] A.C. Grimsdale, K. Leok Chan, R.E. Martin, P.G. Jokisz, A.B. Holmes, Chemical Reviews 109 (2009) 897–1091.

[7] Q. Hou, Y. Xu, W. Yang, M. Yuan, J. Peng, Y. Cao, Journal of Materials Chemistry 12 (2002) 2887–2892.
[8] Y.J. Cheng, S.H. Yang, C.S. Hsu, Chemical Reviews 109 (2009) 5868–5923.
[9] P.M. Beaujuge, C.M. Amb, J.R. Reynolds, Accounts of Chemical Research 43 (2010) 1396–1407.
[10] R. Kroon, M. Lenes, J.C. Hummelen, P.W.M. Blom, B. de Boer, Polymer Reviews 48 (2008) 531–582.
[11] E. Buncel, S. Rajagopal, Accounts of Chemical Research 23 (1990) 226–231.
[12] F. Effenberger, F. Wuerthner, F. Steybe, Journal of Organic Chemistry 60 (1995) 2082–2091.
[13] J. Shao, Z. Guan, Y. Yan, C. Jiao, Q.H. Xu, C. Chi, Journal of Organic Chemistry 76 (2011) 780–790.
[14] D.W. Chang, H.J. Lee, J.H. Kim, S.Y. Park, S.M. Park, L. Dai, J.B. Baek, Organic Letters 13 (2011) 3880–3883.
[15] Z. Ning, H. Tian, Chemical Communications (2009) 5483–5485.
[16] Z.S. Wang, N. Koumura, Y. Cui, M. Takahashi, H. Sekiguchi, A. Mori, T. Kubo, A. Furube, K. Hara, Chemistry of Materials 20 (2008) 3993–4003.
[17] J. Kim, Y.S. Kwon, W.S. Shin, S.J. Moon, T. Park, Macromolecules 44 (2011) 1909–1919.
[18] J. Zhang, W. Cai, F. Huang, E. Wang, C. Zhong, S. Liu, M. Wang, C. Duan, T. Yang, Y. Cao, Macromolecules 44 (2011) 894–901.
[19] S. Kim, J.K. Lee, S.O. Kang, J. Ko, J.H. Yum, S. Fantacci, F. De Angelis, D. Di Censo, M.K. Nazeeruddin, M. Gratzel, Journal of the American Chemical Society 128 (2006) 16701–16707.
[20] J. Hou, H.Y. Chen, S. Zhang, G. Li, Y. Yang, Journal of the American Chemical Society 130 (2008) 16144–16145.
[21] E. Bundgaard, F.C. Krebs, Macromolecules 39 (2006) 2823–2831.
[22] E. Wang, L. Hou, Z. Wang, Z. Ma, S. Hellstro m, W. Zhuang, F. Zhang, S.O. Ingana, M.R. Andersson, Macromolecules 44 (2011) 2067–2073.
[23] M.F. Falzon, M.M. Wienk, R.A.J. Janssen, Journal of Physical Chemistry C 115 (2011) 3178–3187.
[24] Y. Lee, T.P. Russell, W.H. Jo, Organic Electronics 11 (2010) 846–853.
[25] N. Blouin, A. Michaud, D. Gendron, S. Wakim, E. Blair, R. Neagu-Plesu, M. Belletête, G. Durocher, Y. Tao, M. Leclerc, Journal of the American Chemical Society 130 (2008) 732–742.
[26] M.T. Lloyd, J.E. Anthony, G.G. Malliaras, Materials Today 10 (2007) 34–41.
[27] B. Walker, C. Kim, T.Q. Nguyen, Chemistry of Materials 23 (2011) 470–482.
[28] J. Zhang, D. Deng, C. He, Y. He, M. Zhang, Z.G. Zhang, Z. Zhang, Y. Li, Chemistry of Materials 23 (2011) 817–822.
[29] F. Silvestri, M.D. Irwin, L. Beverina, A. Facchetti, G.A. Pagani, T.J. Marks, Journal of the American Chemical Society 130 (2008) 17640–17641.
[30] J. Li, Q. Li, D. Liu, ACS Applied Materials and Interfaces 3 (2011) 2099–2107.
[31] Y. Li, A.Y. Li, B.X. Li, J. Huang, L. Zhao, B.Z. Wang, J.W. Li, X.H. Zhu, J. Peng, Y. Cao, Organic Letters 11 (2009) 5318–5321.
[32] Y. Yang, Y. Zhou, Q. He, C. He, C. Yang, F. Bai, Y. Li, Journal of Physical Chemistry B 113 (2009) 7745–7752.
[33] J.L. Wang, Y. Zhou, Y. Li, J. Pei, Journal of Organic Chemistry 74 (2009) 7449–7456.
[34] B. Walker, A.B. Tamayo, X.D. Dang, P. Zalar, J.H. Seo, A. Garcia, M. Tantiwiwat, T.Q. Nguyen, Advanced Functional Materials 19 (2009) 3063–3069.
[35] J. Roncali, P. Frere, P. Blanchard, R. de Bettignies, M. Turbiez, S. Roquet, P. Leriche, Y. Nicolas, Thin Solid Films 511 (2006) 567–575.
[36] X. Sun, Y. Zhou, W. Wu, Y. Liu, W. Tian, G. Yu, W. Qiu, S. Chen, D. Zhu, Journal of Physical Chemistry B 110 (2006) 7702–7707.
[37] M. Lloyd, A. Mayer, A. Tayi, A. Bowen, T. Kasen, D. Herman, D. Mourey, J. Anthony, G. Malliaras, Organic Electronics 7 (2006) 243–248.
[38] P. Shen, G. Sang, J. Lu, B. Zhao, M. Wan, Y. Zou, Y. Li, S. Tan, Macromolecules 41 (2008) 5716–5722.
[39] F. Wang, J. Luo, K. Yang, J. Chen, F. Huang, Y. Cao, Macromolecules 38 (2005) 2253–2260.
[40] D.A.M. Egbe, T. Kietzke, B. Carbonnier, D. Mühlbacher, H.H. Hörhold, D. Neher, T. Pakula, Macromolecules 37 (2004) 8863–8873.
[41] W. Tang, L. Ke, L. Tan, T. Lin, T. Kietzke, Z.K. Chen, Macromolecules 40 (2007) 6164–6171.
[42] L. Huo, Z. Tan, X. Wang, Y. Zhou, M. Han, Y. Li, Journal of Polymer Science Part A: Polymer Chemistry 46 (2008) 4038–4049.
[43] R. Yang, R. Tian, J. Yan, Y. Zhang, J. Yang, Q. Hou, W. Yang, C. Zhang, Y. Cao, Macromolecules 38 (2005) 244–253.
[44] J.H. Yum, D.P. Hagberg, S.J. Moon, K.M. Karlsson, T. Marinado, L. Sun, A. Hagfeldt, M.K. Nazeeruddin, M. Gratzel, Angewandte Chemie International Edition 121 (2009) 1604–1608.
[45] D.P. Hagberg, J.H. Yum, H.J. Lee, F. De Angelis, T. Marinado, K.M. Karlsson, R. Humphry-Baker, L. Sun, A. Hagfeldt, M. Gratzel, Journal of the American Chemical Society 130 (2008) 6259–6266.
[46] I.M. Downie, M.J. Earle, H. Heaney, K.F. Shuhaibar, Tetrahedron 49 (1993) 4015–4034.
[47] O. Meth-Cohn, D.L. Taylor, Journal of the Chemical Society, Chemical Communications (1995) 1463–1464.
[48] P. Wei, X. Bi, Z. Wu, Z. Xu, Organic Letters 7 (2005) 3199–3202.
[49] H. Zhang, B. Yang, Y. Zheng, G. Yang, L. Ye, Y. Ma, X. Chen, G. Cheng, S. Liu, Journal of Physical Chemistry B 108 (2004) 9571–9573.
[50] E. Grabiec, M. Kurcok, E. Schab-Balcerzak, Journal of Physical Chemistry A 113 (2009) 1481–1488.
[51] J.A. Hur†, S.Y. Bae, K.H. Kim, T.W. Lee, M.J. Cho, D.H. Choi, Organic Letters 13 (2011) 1948–1951.
[52] S. Janietz, D. Bradley, M. Grell, C. Giebeler, M. Inbasekaran, E. Woo, Applied Physics Letters 73 (1998) 2453.
[53] J.J.A. Chen, T.L. Chen, B.S. Kim, D.A. Poulsen, J.L. Mynar, J.M.J. Fre chet, B. Ma, ACS Applied Materials and Interfaces 2 (2010) 2679–2686.
[54] C. Reichardt, Chemical Reviews 94 (1994) 2319–2358.
[55] A. Kapturkiewicz, J. Herbich, J. Karpiuk, J. Nowacki, Journal of Physical Chemistry A 101 (1997) 2332–2344.
[56] A.M. Sarker, E.E. Gürel, M. Zheng, P.M. Lahti, F.E. Karasz, Macromolecules 34 (2001) 5897–5901.
[57] K.Y. Peng, S.A. Chen, W.S. Fann, S.H. Chen, A.C. Su, Journal of Physical Chemistry B 109 (2005) 9368–9373.
[58] H.P. Rathnayake, A. Cirpan, P.M. Lahti, F.E. Karasz, Chemistry of Materials 18 (2006) 560–566.
[59] J.N. Moorthy, P. Venkatakrishnan, P. Natarajan, D.F. Huang, T.J. Chow, Journal of the American Chemical Society 130 (2008) 17320–17333.